



A new coating filter of coated structure for topology optimization

Gil Ho Yoon¹ · Bing Yi²

Received: 13 December 2018 / Revised: 28 March 2019 / Accepted: 9 April 2019

© Springer-Verlag GmbH Germany, part of Springer Nature 2019

Abstract

The present research develops a new density filter in topology optimization considering the coating structure. The coating structure refers to a uniform thickness structure covering the surface of a substrate structure and it is one of the important manufacturing techniques for the decorative or the functional purpose. In order to find out topological designs with the coating structure, this study develops a new density filter approach by multiplying the modified density design variables and the original design variables. Compared to the other approaches, this density coating filter uses simple averaging or the p -norm of the neighborhood densities to find out the envelope of the substrate, and we propose to multiply the modified densities and the original densities to define the uniformly thick coating layer. By modifying the radius of the envelope, it is possible to modify the thickness of the coating layer. Several numerical examples are presented to demonstrate the validity and effectiveness of the present coating filter scheme.

Keywords Topology optimization · Coating · Density filter · p -norm approach

1 Introduction

This paper presents a new coating filter in the topology optimization framework by combining the modified density design variables and the original design variables. Figure 1 sketches the substrate and the coating structure at the surface of the substrate of interest for the decorative or functional purpose (Møller and Nielsen 2013; Shchukin and Möhwald 2013). The coating structure can be found in many engineering application areas. After engineers design the substrate structures without considering the effects of the coating, additional materials are deposited, painted, or added with a controlled thickness using a simple brushing or an expensive machinery in electronic companies (Møller and Nielsen 2013; Shchukin and Möhwald 2013). To consider

this coating issue from structural optimization viewpoint, we can regard the coating and its design as a manufacturing constraint and can consider the effect of the coating layer on stiffness. In other words, it may be possible to design a mechanical system considering the effect of the coating (Deaton and Grandhi 2014). This paper presents a new coating filter to find out an optimal substrate structure and the coating layer with a controlled thickness by combining the existing filtering techniques. To prove the concept of the present approach, several topology optimization examples are solved.

After the development of the concept of topology optimization, several creative innovative structural optimization methods such as the SIMP (solid isotropic material with penalization), the level-set approach, the moving morphable component, the element connectivity parameterization approach, and the deep learning-based approach have been developed (Bendsøe and Kikuchi 1988; Wang et al. 2003; Xia et al. 2012; Zhang et al. 2018; Moon and Yoon 2013; Yu et al. 2019). Without the a priori given optimal topology, the topology optimization scheme can provide new and unanticipated optimal layouts for complex engineering structures, and has been widely applied for multiphysics systems (Yoon 2010; Jensen and Sigmund 2011; Yoon 2016; Evgrafov et al. 2008; Papoutsis-Kiachagias and Giannakoglou 2016; Yoon 2012; Deaton and Grandhi 2014; Ha and Cho 2005; Alexandersen et al. 2012; Dede et al. 2014; Tsuji et al. 2006; Xie and Steven 1993; Zhang et al.

Responsible Editor: Ji-Hong Zhu

Electronic supplementary material The online version of this article (<https://doi.org/10.1007/s00158-019-02279-7>) contains supplementary material, which is available to authorized users.

✉ Gil Ho Yoon
ghy@hanyang.ac.kr; gilho.yoon@gmail.com

¹ School of Mechanical Engineering, Hanyang University, Seoul, Republic of Korea

² School of Traffic and Transportation Engineering, Central South University, Changsha, China

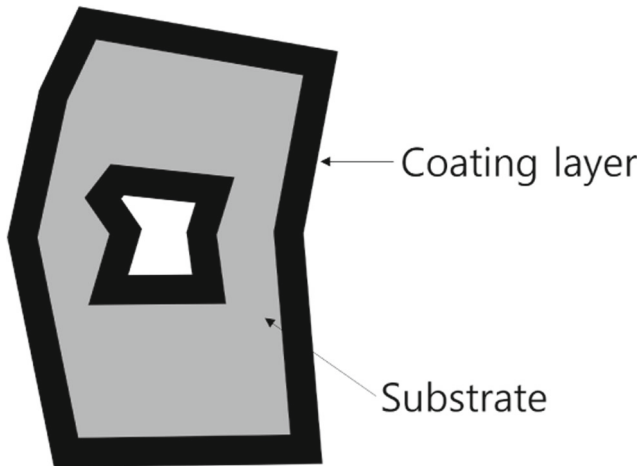


Fig. 1 A coating structure (coating and substrate layers); the tribological properties of a substrate, as well as the stiffness, can be improved with surface coating

2018; Yoon 2014; Xia et al. 2012). In topology optimization, the design variables assigned to each cell or the elements of the finite element models or the finite element volume interpolate the material properties of the physical equations of interest. The most straightforward interpolation scheme is the SIMP scheme (Bendsøe and Kikuchi 1988). Inspired by the pioneer studies (Clausen et al. 2015; Wang and Kang 2018; Yoon 2013), the present study tries to contribute a topology optimization research considering the uniform coating layer.

The coating techniques in tribology are intriguing subjects for exploration in their own right, but the impetus for investigating the microstructure and developing innovative materials comes mainly from the vision of innovative materials/structures and bio-inspired materials. With the help of the coating technology, a structure with automatic functionality called smart coating was proposed (Shchukin and Möhwald 2013). An ultralight metallic material was developed from the polymer as a complex substructure (Schaedler et al. 2011). With a recent development in 3D printing technology or additive manufacturing technology, the bone-like structure and hollow-shell structure can be manufactured (Tofail et al. 2018; Wang et al. 2005). Wang et al. (2013) presented a new method for inner truss optimization based on sparsity analysis. Lu et al. (2014) presented a hollowing optimization method based on the Voronoi diagram for an optimal interior tessellation with a large strength-to-weight ratio. Clausen et al. (2015) proposed an optimization method considering the coated structure with a solid shell and an inner uniform lattice structure. Wu et al. presented a density-based optimization method with a local volume constraint to design both the coating and the infill structure to minimize the compliance of the structure using the gradient norm-based

coating structure (Wu et al. 2018; Wu et al. 2017). The computation of the gradient is complex, and exactly approximating the maximum of the gradient norm may be difficult. An efficient level-set-based method with the coating layer and a shell-infill structure was developed (Wang and Kang 2018; Fu et al. 2019; Fu et al. 2019). The coating structure or technology also provides an innovative approach to mitigate the mechanical merits of substrate and coating structures to make a cost-effective structure. For instance, it was mentioned that bone-like structure, in-fill structure, or hollow-shell structure can be regarded as a coating structure. Furthermore, with the development of additive manufacturing technology, complex structures can be fabricated (Wang and Kang 2018).

In the present study, the thickness of the coating layer is on the order of that of the substrate structure using the topology optimization scheme and the contribution of the coating structures in terms of stiffness is not negligible. Therefore, the topology optimization problems minimizing the compliance subject to the mass constraint and their optimal layouts are influenced by the consideration of the coating structure or the layered structure. To implement this coating idea, this study applies the filtered design variables defining the coating layer in Fig. 2. The idea was first proposed by Yoon (2013) to accommodate the porous material design in an acoustic topology optimization problem. However, the exact sensitivity analysis was not derived and a heuristic approach in optimization was employed. In the present study, we expand the concept and derive the exact sensitivity for the topology optimization problem with the coating.

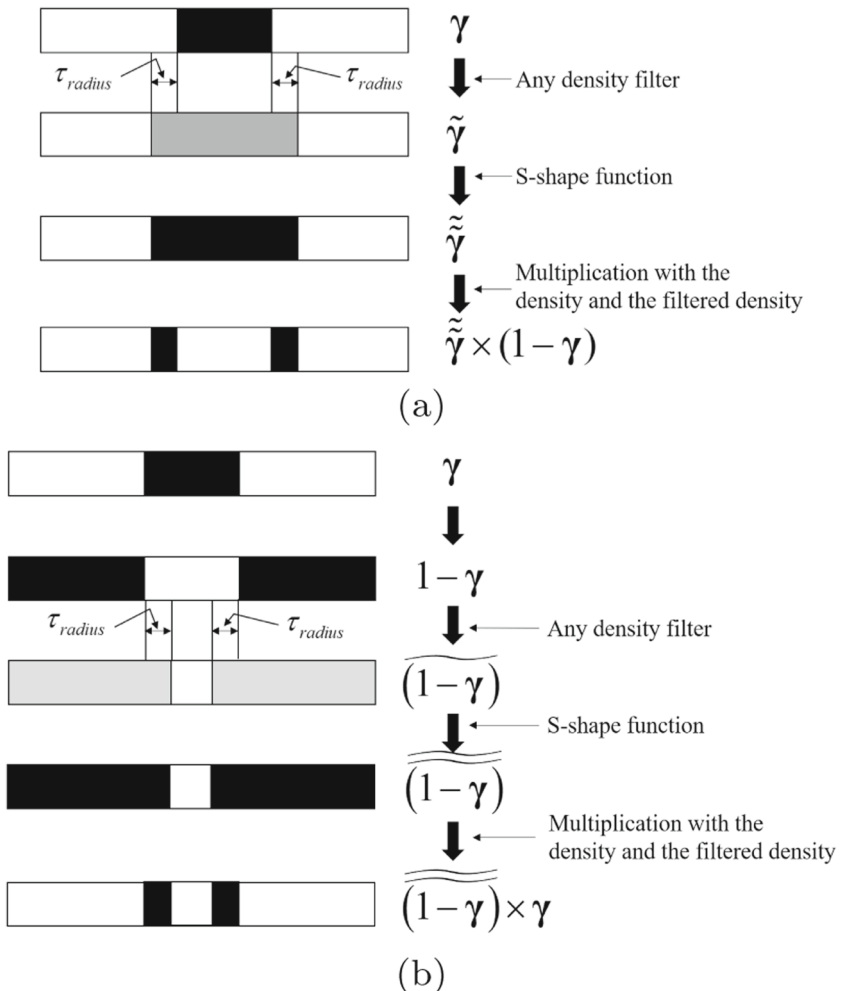
The rest of this paper is organized as follows. Section 2 describes the basic equations for the structural optimization problem. Section 3 develops a new coating filter and discusses its application. Section 4 presents several numerical examples to show the advantages and disadvantages of the present coating filter with topology optimization problems. Section 5 presents the conclusions and suggests future research.

2 A new density filter for the coating structure

2.1 Problem definition: linear elasticity equation and topology optimization

Some optimal layouts that result from the topology optimization mainly considering the performance of the structure subject to several constraints need some postprocessing for the manufacturing (Li et al. 2016; Sato et al. 2017; Langelaar 2016). A topologically optimized design can contain somehow complicated geometric features to be

Fig. 2 A new density coating filter. **a** The outer coating filter operator and **b** the inner coating filter operator



manufactured through viable manufacturing techniques or can be too expensive to be manufactured. Indeed, some geometrical modifications of the native optimal layouts by the topology optimization scheme are required, which can degrade the performance significantly. Therefore, the local or global geometrical constraints should be added in the formulation of the topology optimization but this poses obstacles to the realization of successful and stable mathematical formulations.

To develop a coating density filter, the topology optimization problem minimizing compliance subject to the mass constraint is considered here with the SIMP interpolation function. The governing equation for solving the equilibrium equation on the domain Ω is given as follows:

$$\nabla \cdot \boldsymbol{\sigma}(\mathbf{u}) + \mathbf{b} = \mathbf{0} \text{ in } \Omega \quad (1)$$

where the Cauchy stress tensor, displacement vector, and body force are denoted by $\boldsymbol{\sigma}$, \mathbf{u} , and \mathbf{b} , respectively. The Neumann boundary condition alongside $\partial\Omega_N$ and the

Dirichlet boundary condition alongside $\partial\Omega_D$ are described as follows:

$$\begin{aligned} \boldsymbol{\sigma} \cdot \mathbf{n} &= \mathbf{f} \text{ on } \partial\Omega_N \\ \mathbf{u} &= \mathbf{0} \text{ on } \partial\Omega_D \end{aligned} \quad (2)$$

where \mathbf{f} and \mathbf{n} denote the surface traction and the unit normal vector. The constitutive matrix is denoted by \mathbf{C} . The linear strain $\boldsymbol{\epsilon}$ and stress $\boldsymbol{\sigma}$ relation are assumed.

$$\boldsymbol{\sigma} = \mathbf{C}\boldsymbol{\epsilon} \quad (3)$$

The finite element procedure is applied for computing structural displacements. After that, the following topology optimization problem can be formulated.

$$\begin{aligned} \text{Min}_{\gamma} &= \mathbf{F}^T \mathbf{U} \\ \text{Subject to } &V(\hat{\gamma}, \gamma) \leq V^0 \\ \mathbf{K}(\hat{\gamma}, \gamma) \mathbf{U} &= \mathbf{F}, \hat{\gamma} = \Phi(\gamma) \\ \Phi : \text{Coating filter}, \gamma &= [\gamma_1, \gamma_2, \gamma_3 \dots \gamma_{nel}] \end{aligned} \quad (4)$$

where the stiffness matrix, displacement, and force vectors are denoted as \mathbf{K} , \mathbf{U} , and \mathbf{F} , respectively. The filtered design

variable with the coating density filter is denoted by $\hat{\gamma}$ and the number of design variable is denoted by nel . The mass of the substrate and the allowed maximum mass are denoted by V and V^0 , respectively. The independent mass constraint for the coating mass is hard to consider with a gradient optimizer as the coating structure only appears when the substrate exists. Furthermore, the perimeter of the substrate structure determines the mass of the coating layer. Note that the mass of the substrate is constrained as the present study tries to model coating as protected layers. In case of shell-infill or infill lattice, the masses of the substrate and the coating become important. Solving the compliance minimization problem considering the coating structure, the mass constraint should be carefully formulated. In the present study, the mass constraint for the substrate structure is considered for the constraint of the optimization formulation. Depending on the engineering specifications, it is possible to modify the optimization formulation and the constraint. The above stiffness matrix with the density design variable and the auxiliary variables defining the coating layer can be constructed as follows:

$$\mathbf{K}(\hat{\gamma}(\gamma), \gamma) \mathbf{U} = \mathbf{F}, \mathbf{K}(\hat{\gamma}(\gamma), \gamma) = \sum_{e=1}^{nel} \mathbf{k}_e(\hat{\gamma}_e, \gamma_e) \quad (5)$$

where the element stiffness \mathbf{k}_e is interpolated with the stiffness matrices of the substrate, $\mathbf{k}_{substrate}$, and the coating layer, $\mathbf{k}_{coating}$, as follows:

$$\mathbf{k}_e(\hat{\gamma}_e, \gamma_e) = \mathbf{k}_{substrate} \gamma_e^n + \mathbf{k}_{coating} \hat{\gamma}_e^{n_c} \quad (6)$$

The penalization factors of SIMP are denoted by n and n_c . Then, the determination of $\hat{\gamma}_e$ satisfying the non-overlapping area with the area of the substrate structure and the uniform thickness layer on the surface of the substrate structures is important for topology optimization with the coating layer. To enable the use of a gradient-based optimizer, the sensitivity values of the objective and the constraint with respect to the e th design variable can be computed as follows:

$$\frac{dc}{d\gamma} = \frac{\partial c}{\partial \gamma} + \frac{\partial c}{\partial \hat{\gamma}} \frac{\partial \hat{\gamma}}{\partial \gamma} \quad (7)$$

$$\frac{\partial c}{\partial \gamma} = -\mathbf{U}^T \frac{\partial \mathbf{K}}{\partial \gamma} \mathbf{U}, \frac{\partial c}{\partial \hat{\gamma}} = -\mathbf{U}^T \frac{\partial \mathbf{K}}{\partial \hat{\gamma}} \mathbf{U} \quad (8)$$

$$\frac{dV}{d\gamma} = \frac{\partial V}{\partial \gamma} + \frac{\partial V}{\partial \hat{\gamma}} \frac{\partial \hat{\gamma}}{\partial \gamma} \quad (9)$$

The above gradient values can be efficiently obtained with any differential density filter. Then, the optimization problem can be solved with a finite element strategy using a gradient-based optimizer. For the topology optimization, it is crucial to interpolate the material properties with respect to the continuous density variable in the SIMP method to avoid the discrete 0-1(void or solid) optimization problem.

2.2 A new density filter for external coating

On the basis of the multimaterial interpolation in topology optimization modified for the geometry constraint for the coating in Fig. 2, we propose to interpolate the element stiffness matrix with respect to the design variable in (10).

$$\begin{aligned} \mathbf{k}_e(\hat{\gamma}_e, \gamma_e) &= \mathbf{k}_{substrate} \cdot \gamma_e^n + \mathbf{k}_{coating} \cdot \{\hat{\gamma}_e\}^{n_c} \\ \hat{\gamma}_e &= \left\{ \tilde{\gamma}_e \times (1 - \gamma_e) \right\} \\ \mathbf{k}_e(\hat{\gamma}_e, \gamma_e) &= \mathbf{k}_{substrate} \cdot \gamma_e^n + \mathbf{k}_{coating} \cdot \left\{ \tilde{\gamma}_e \times (1 - \gamma_e) \right\}^{n_c} \end{aligned} \quad (10)$$

where the e th element stiffness matrix, substrate-element stiffness matrix, and coating-element stiffness matrix are denoted by \mathbf{k}_e , $\mathbf{k}_{substrate}$, and $\mathbf{k}_{coating}$, respectively. The two penalization factors, i.e., n and n_c , are employed for SIMP penalization factors. The penalization factor n is set to a real value higher than 3 and the factor n_c is set to a real value higher than 7. One of the unique features of the present interpolation function in (10) is that the combination of the filtered design variable and the original design variable defines the stiffness matrix. The e th design variable, γ_e , determines whether a material exists at the corresponding spatial finite element. The auxiliary design variables, $\hat{\gamma}_e$, determine the existence of the coating layer; $\tilde{\gamma}_e$ will be defined later. The idea using the above interpolation function was originally proposed (Yoon 2013) but with the heuristic sensitivity analysis. This study derives the exact sensitivity for the compliance minimization problem considering the coating layer. Depending on the requirement, we can manipulate the combinations to develop the coating layer in topology optimization.

Now, the formulation defining $\tilde{\gamma}_e$ will be presented. The variable $\tilde{\gamma}_e$ should be ones (solid or coating) inside the constant-radius offset with a distance of the coating thickness of a substrate structure defined by γ and zeros (void) elsewhere. For this purpose, we propose to use the following nonlinear mapping with the density filter.

$$\begin{aligned} \text{Density filter : } \tilde{\gamma} &= \Phi_{Outer}(\gamma) \\ s - \text{shape function: } \tilde{\gamma} &= \Psi_s(\tilde{\gamma}) = \frac{1}{(1 + \exp(a(\tilde{\gamma} - b)))} \end{aligned} \quad (11)$$

For the density filter, the following average filter, the weight sum filter, and the p -norm filter are proposed and tested here.

$$\text{Average filter: } \Phi_{Outer}(\gamma) = \frac{\sum_{e \in Neighbor} \gamma_e}{N_{neighbor}} \quad (12)$$

$$\begin{aligned} \text{Weight sum filter: } \Phi_{Outer}(\gamma) &= \frac{\sum_{e \in Neighbor} w_e \times \gamma_e}{\sum_{e \in Neighbor} w_e} \\ w_e &= \text{distance} \end{aligned} \quad (13)$$

$$p\text{-norm filter: } \Phi_{Outer}(\gamma) = \left(\sum_{e \in Neighbor} \gamma_e^p \right)^{\frac{1}{p}} \quad (14)$$

where the set of neighbor elements of the e th element inside a circle with a τ_{radius} radius is denoted by $Neighbor$ and the number of the neighbor elements is $N_{neighbor}$. After these density filter processes, the s -shape function's main purpose is to develop the filtered design variables $\tilde{\gamma}$ to ones or zeros (Yoon and Kim 2003). Any s -shape function can be employed and this study employed the function with the exponent in (11) with the parameters a determining the slope of the curve and b determining the cutoff value (Yoon and Kim 2003). For example, we consider the 180×180 pixel image in Fig. 3a containing thin lines, thick lines, circles, cup, and triangles. First, the coating filter with the combination of the average filter and the s -shape function is tested. The coating structures appear in Fig. 3b–d with some different parameters of the s -shape function. As illustrated in Fig. 3, the coating structures with unique thickness can be observed. With the averaging density filter, a smaller value should be used for the cutoff value, b . Figure 4 shows the application for the weighting sum filter. Note that, unlike the weight averaging filter for topology optimization, the weight values are set to the distance values meaning that the design variables far from the center are emphasized. With the averaging density filter, a smaller value should be used for the cutoff value, b .

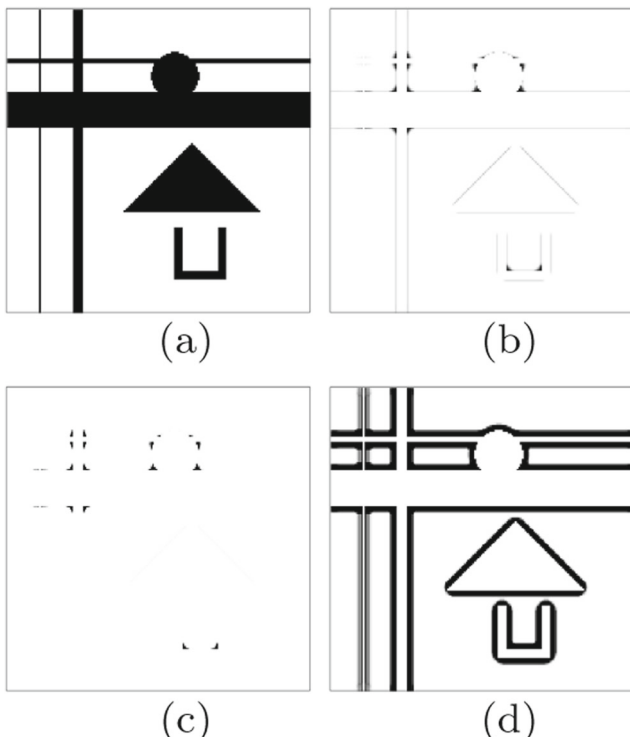


Fig. 3 Example of the present coating filter. **a** An original 180×180 pixel layout, the coating (averaging filter) with $\tau_{radius} = 5$ pixels with **b** $a = -30, b = 0.5$, **c** $a = -90, b = 0.5$, and **d** $a = -90, b = 0.1$

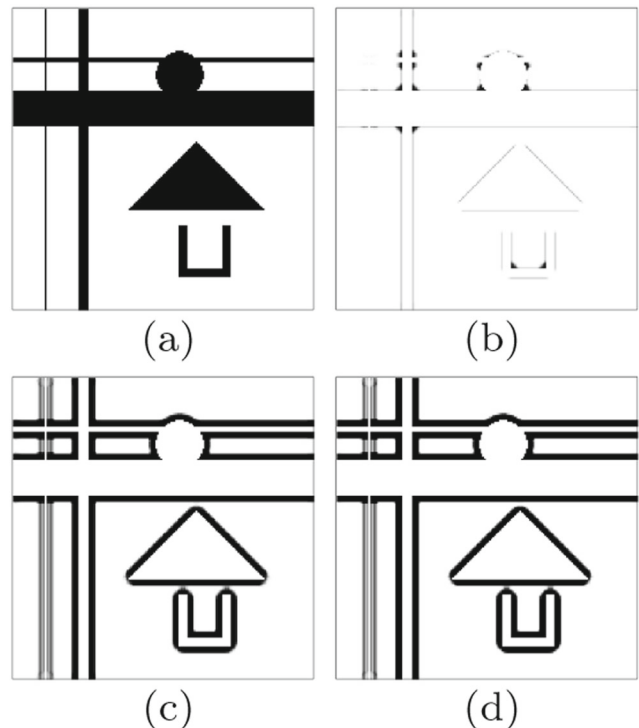


Fig. 4 Example of the present coating filter. **a** An original 180×180 pixel layout, the coating (weight sum filter) with $\tau_{radius} = 5$ pixels with **b** $a = -30, b = 0.5$, **c** $a = -60, b = 0.1$, and **d** $a = -90, b = 0.1$

possible to use the p -norm to find out the envelope of the design variable. Originally, the p -norm was used to find out the approximated maximum stress values in topology optimization. Recently, the application of this p -norm in the density filter was proposed (Langelaar 2018). Figure 5 shows the coating structures with the p -norm of the density variables. As the p -norm of the design variables in (14) is an approximated maximum density, the coating filter is robust to parameters a and b . To show the detailed procedure of Fig. 2a, the intermediate processes are plotted in Fig. 6 with the p -norm approach.

2.3 Extension for the internal coating

In the above subsection, the coating filter was newly developed. One of the geometrical constraints of the developed filter is that the coating structure appears at the outer surface of the substrate structure. As an extension of this filter, the inner coating filter can be defined by modifying the above filter. In other words, rather than applying the density filter to γ for the coating layer, the density filter can be applied to $1 - \gamma$ to define the coating layer. As the filtered values define the inner envelope, it can be used for the coating layer defined inside the structure. The other processes are identical to those of the

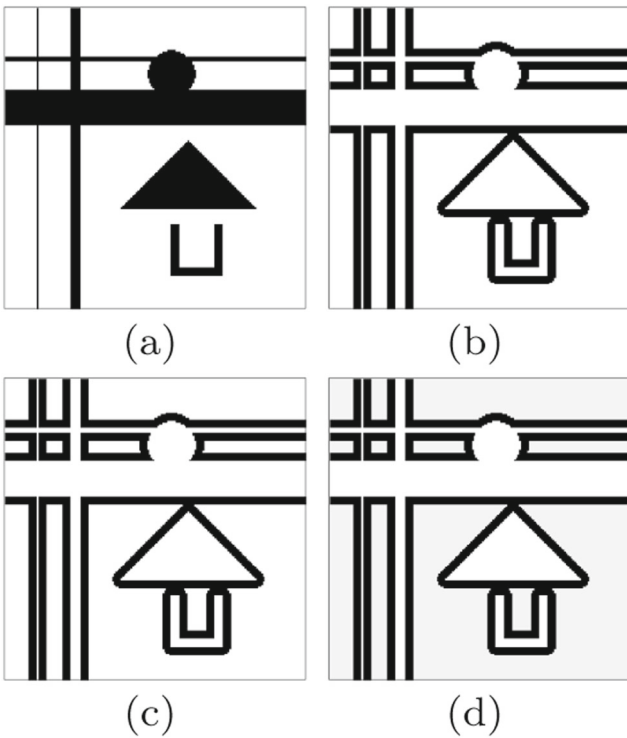


Fig. 5 Example of the present coating filter. **a** An original 180×180 pixel layout, the coating (p -norm filter) with $\tau_{radius} = 5$ pixels $p = 5$ with **b** $a = -30, b = 0.5$, **c** $a = -60, b = 0.5$, and **d** $a = -30, b = 0.1$

outer coating filter and the interpolation formulation can be summarized as follows:

$$\mathbf{k}_e(\hat{\gamma}_e, \gamma_e) = \mathbf{k}_{structure} \cdot \gamma_e^n + \mathbf{k}_{coating} \cdot \{\hat{\gamma}_e\}^{n_c}$$

$$\hat{\gamma}_e = (\tilde{\gamma})^{\frac{1}{n_c}} \times \gamma_e \quad (15)$$

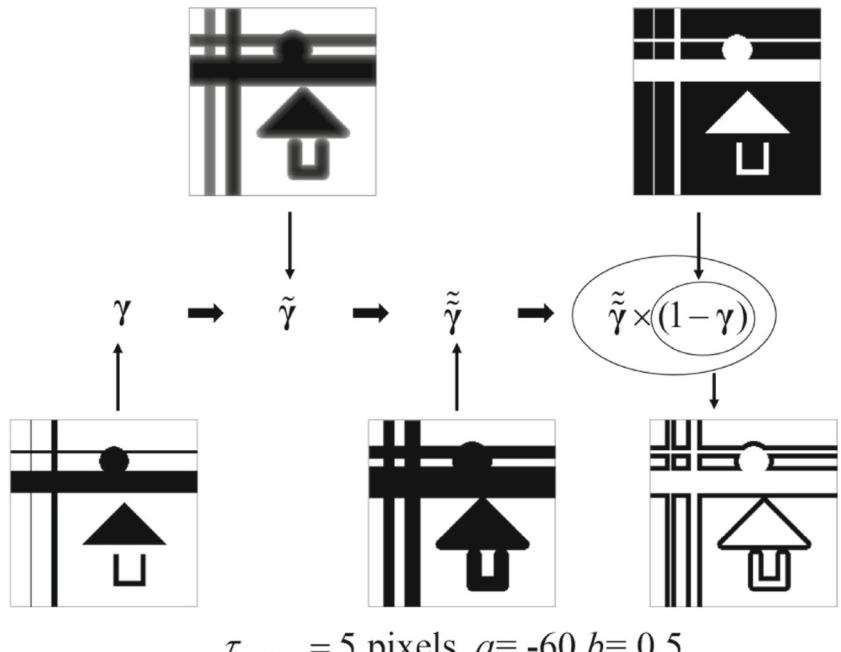
Fig. 6 Detailed procedure of Fig. 5(c)

Figure 7 shows the layout obtained by the inner coating filter with the original image. For a member thinner than 5 pixels, the inner coating structure occupies the member, while for a member thicker than 5 pixels, the offset structure appears. Therefore, it is possible to consider this filter to find out an optimal layout with the inner coating structure.

To test the present filter with gray elements (between 0 and 1), Fig. 8 shows the images filtered by the outer filter and the inner filter (the p -norm filter with $a = -60$ and $b = 0.5$) with the image with gray values. With the intermediate design variables, the coating filter can successfully define the coating layer. When the design variables have small values, i.e., at the top of the triangle, the coating layer does not appear.

2.4 Optimality condition for the coating structure

The changes in the optimal layouts considering the uniform coating structure or the layered structure should be considered. Not to mention, as the coating structure of a given structure will contribute to the stiffness of the integrated structure (the substrate and the coating layer), the optimality condition or the optimal layout may be subject to a change. The changes in terms of layout or overall stiffness value can be dramatic with a large compliance ratio, i.e., the stiffness ratio of the representative stiffness values of the coating structure to the substrate structure. On the other hand, the changes may be marginal with a small ratio. In the case of marginal difference, it may be possible to conduct the structural optimization neglecting the contributions of the stiffness of the coating structure and the uniform coating structure can be added later alongside the substrate



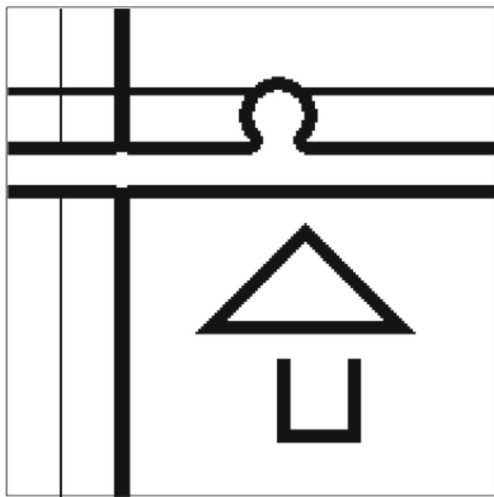


Fig. 7 Example of the inner coating (p -norm filter with $\tau_{radius} = 5$ pixels with $a = -30$, $b = 0.5$)

structure. If the stiffness contribution of the coating structure is significant, the analysis considering the geometrical constraints of the coating and the stiffness contribution should be conducted. The stiffness values of the substrate and coating structures are a function of Young's modulus, Poisson's ratio, and geometric thickness values, and the strong structure should sometimes appear internally to minimize the compliance or maximize the stiffness for a given

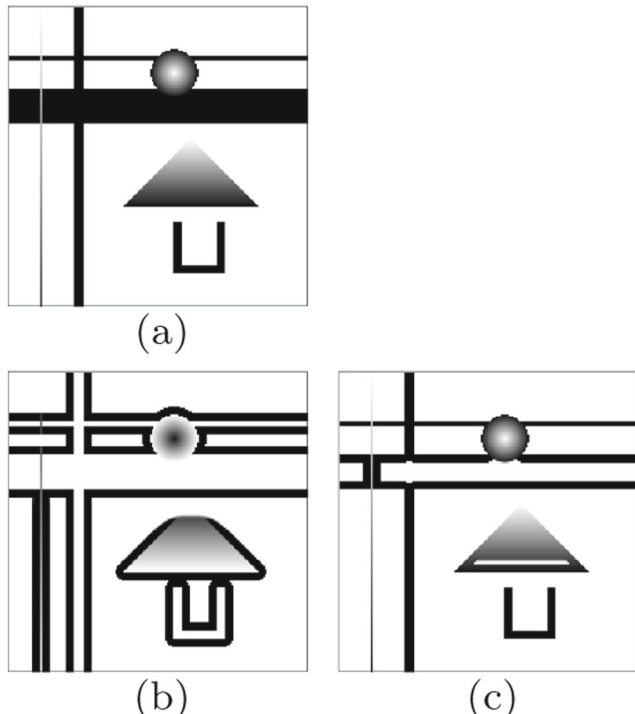


Fig. 8 Example with gray elements. **a** An original 180×180 pixel layout, **b–c** images with the outer and inner coating filters (p -norm filter with $a = -60$, $b = 0.5$)

load. This implies that the optimization problem should consider not only the stiffness but also the geometrical condition, i.e., the coating structure should appear at the outer boundary of the hosting structure. A more adequate explanation of this aspect is to consider a simple conceptual optimization example with the structure in Fig. 9 to determine the optimal material distributions of the weak and strong materials for a simple clamped boundary condition and the point tension force condition. The structures that have the mass ratio do not necessarily have the same compliance. Indeed, if we pursue the global optimum minimizing the compliance subject to the mass constraint without any local or global geometrical condition, the structure whose internal structure is filled with the strong material (Fig. 9(b:right)) becomes the optimal layout in case of the tension or the compression loads. With the bending load, the structure whose outer structure is filled with the strong material (Fig. 9(c:left)) becomes the optimal layout; note that the stiffness values can be changed depending on the

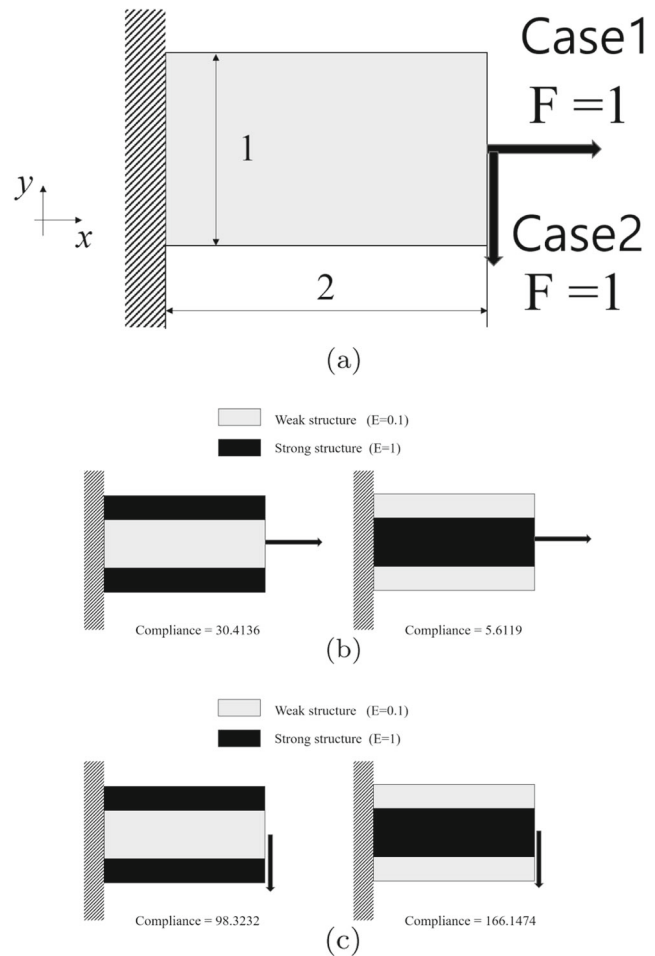


Fig. 9 **a** Compliance comparison with strong material (50 %) and weak material (50 %), **b** comparison with case 1, and **c** comparison with case 2 (for the compliance minimization problem, a lower compliance is achieved with a strong material inside)

moduli and the coating thickness of the coating and substrate materials. We claim that this aspect influences the topology optimization considering the coating. With the stiffness of the coating structure smaller than that of the hosting structure, the tension force is mainly supported by the substrate structure, while the coating structure appears alongside the substrate structure. However, when the stiffness of the coating structure is larger than that of the hosting structure, we observe the opposite situation, i.e., the coating structure becomes an internal structure bearing the load and the hosting structure should be an auxiliary structure.

To have an optimum structure whose hosting structure appears internally and the coating structure appears alongside the hosting structure, an additional constraint or penalization is needed. With a large stiffness of the coating structure, we propose the following continuation interpolation function.

$$\begin{aligned} \mathbf{k}_e(\gamma_e) = & \mathbf{k}_{substrate} \cdot \gamma_e^n + \mathbf{k}_{coating} \cdot \left\{ \tilde{\gamma}_e \cdot (1 - \gamma_e) \right\}^{n_c} \\ & \times \left(\min \left(1, \frac{\text{Optimization Iteration}}{\text{Normalization Factor}} \right) \right)^{n_{iter}} \end{aligned} \quad (16)$$

For n_{iter} , a real value between 3 and 5 gives reasonable results. The normalization factor is set to the maximum optimization iteration.

3 Optimization results

To prove the concept of the present coating scheme, this section solves two-dimensional compliance minimization problems with the coating layer. To check whether the

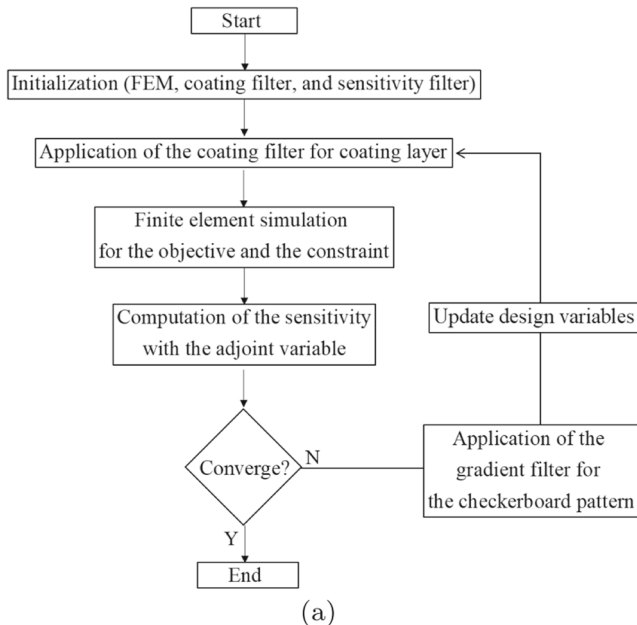


Fig. 10 An optimization procedure

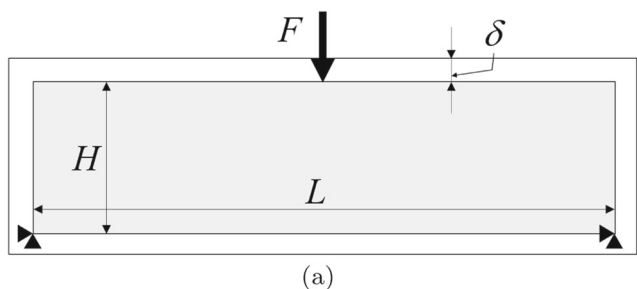


Fig. 11 A rectangular box with a point load ($L=4$ m, $H=1$ m, thickness = 1 m, $\delta=0.16666$ m, $F=2$ N, densities of the substrate and the coating = 1 kg/m^3)

present scheme can successfully coat a substrate structure with the prescribed coating thickness, different thickness values for the coating layer are also tested here. With a larger Young modulus and a larger thickness of the coating layer, the stiffness value of the coating layer influences the optimal layout dramatically. All finite elements and the optimization are implemented in the framework of MatLab. To solve the optimization problem, the method of moving asymptotes (MMA) algorithm is used (Svanberg 1987). Note that the

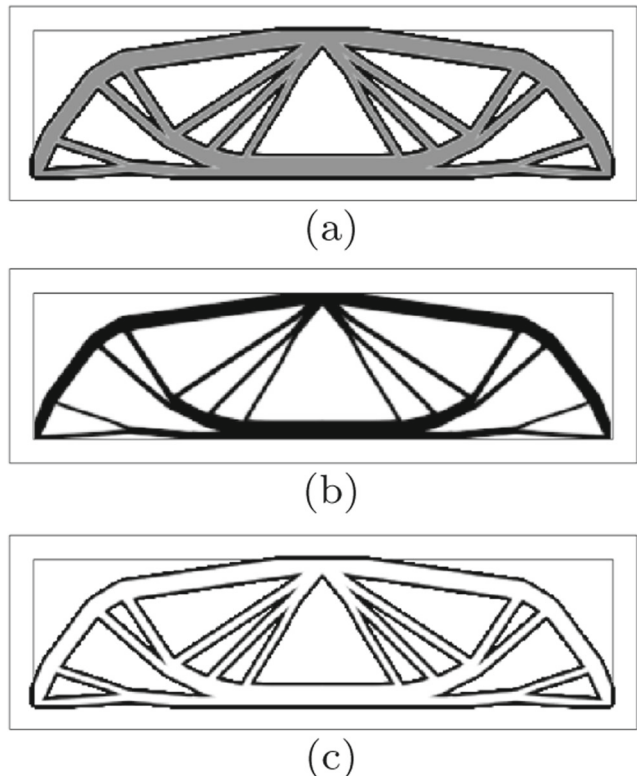
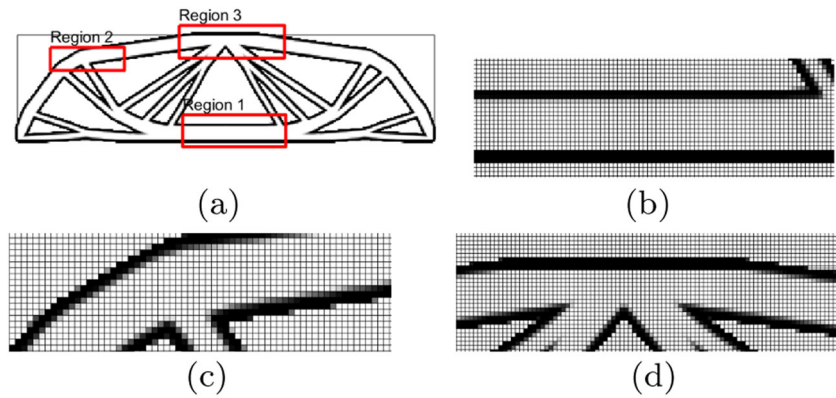


Fig. 12 The optimization result with 3-pixel coating and $E_{coating}=0.1 \text{ N/m}^2$; **a** optimized design (compliance= 117.2621 J (107.9951 J for the substrate and 9.2670 J for the coating layer), $E_{substrate}=1 \text{ N/m}^2$, $E_{coating}=0.1 \text{ N/m}^2$, $p=6$, $a=-30$, $b=0.5$, $V^0=30\%$, the mass of the coating= 21.7881 %), **b** the substrate structure, and **c** the coating structure (coating thickness= 0.0333 m or 3 pixels)

Fig. 13 Details of Fig. 12 with the coating with 3 pixels: **a** regions of interest, **b** detail of region 1, **c** detail of region 2, and **d** detail of region 3



original design variable γ defines the substrate and the auxiliary design variable $\hat{\gamma}$ defines the coating layer around the substrate. The present study uses the gradient filter with the radius $1.5 \times$ element size to remove the checkerboard pattern. The overall procedure is illustrated in Fig. 10.

3.1 Example 1: a rectangular box with a point load

First, the problem (a rectangular domain with a point load) in Fig. 11 is considered. The design domain ($4\text{ m} \times 1\text{ m}$) for the substrate structure is discretized by 360×90 linear plane stress finite elements with the extended domain offsetting the design domain with a uniform distance (0.1667 m or 15 finite elements) for the coating structure. This uniform coating thickness layer is added to allow the development or appearance of the coating structure when the substrate material appears near the boundary of the design domain (the internal area in Fig. 11).

Figure 12a shows the optimal layout with 117.2621 J for the problem with the uniform thickness coating layer with 0.0333 m line width or 3 pixels of the finite elements. To represent the substrate structure and the coating structure simultaneously, the substrate structure is rendered by gray color and the coating structure is rendered by black color in Fig. 12a. Figure 12b and c separately plot the substrate structure and coating structure, respectively. Fig. 13 shows the three detailed features of the coating structure in Fig. 12. As illustrated, the uniform-coating-thickness structure (0.0333 m or 3 pixels) can be obtained by the present topology optimization method. Figure 14 shows the convergence history of 500 iterations (normalization factor = 300). The compliance contributions of the substrate structure and the coating structure are also computed and plotted together in Fig. 14b. The optimization process first minimizes the compliance mainly from the substrate structure. In the beginning of the optimization, the effect of the coating layer is diminished with uniform distributions of the design variables. After a few iterations, the coating structure starts to appear and its contribution to the compliance

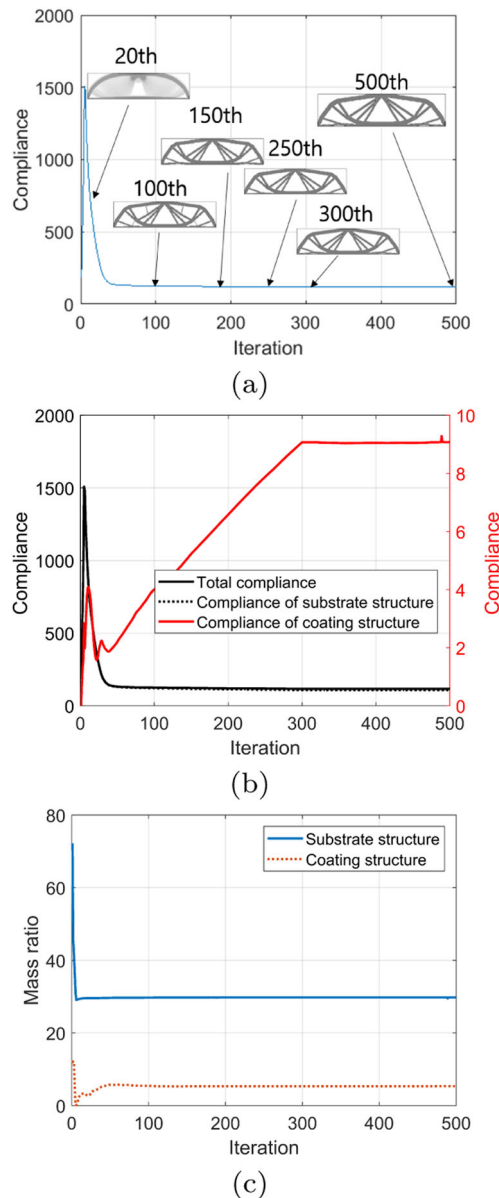


Fig. 14 Optimization history of Fig. 12 with coating thickness= 0.0333 m or 3 pixels

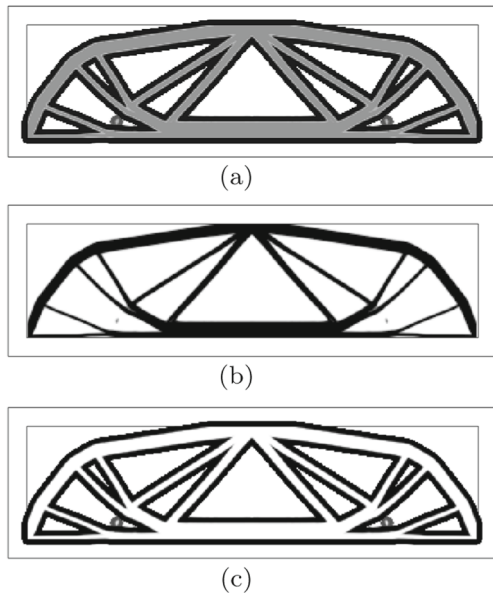


Fig. 15 Optimization result with 5-pixel coating and $E_{coating} = 0.1 \text{ N/m}^2$. **a** The optimized design (compliance= 109.2656 J (94.8433 J for the substrate and 14.4132 J), $E_{substrate}= 1 \text{ N/m}^2$, $E_{coating}= 0.1 \text{ N/m}^2$, $p= 6$, $a= -30$, $b= 0.5$, $V^0= 30\%$, the mass of the coating= 37.4140 %), **b** the substrate structure, and **c** the coating structure (coating thickness=0.0556 m or 5 pixels)

increases. Similar to conventional coating structures used to prevent corrosion with small contributions to the stiffness, the contribution of the coating structure in this example is about 7.9 % (107.9951 J for the substrate and 9.2670 J for the coating layer). Figure 15 shows the optimal layout with uniform-thickness-coating structure (0.0556 m or 5 pixels). Compared to the design in Fig. 12, the overall layout is similar but with a thicker coating structure. Figure 16 shows the detailed geometries of the optimized structure and note that the uniform coating thickness structure appears successfully. Due to the reinforcement of the coating structure, the compliance is also reduced to 109.2656 J (94.8433 J (86.8190 %) for the substrate and 14.4132 J (13.1921 %) for the coating layer).

Fig. 16 Details of Fig. 15 with the coating with 5 pixels: **a** regions of interest, **b** detail of region 1, **c** detail of region 2, and **d** detail of region 3

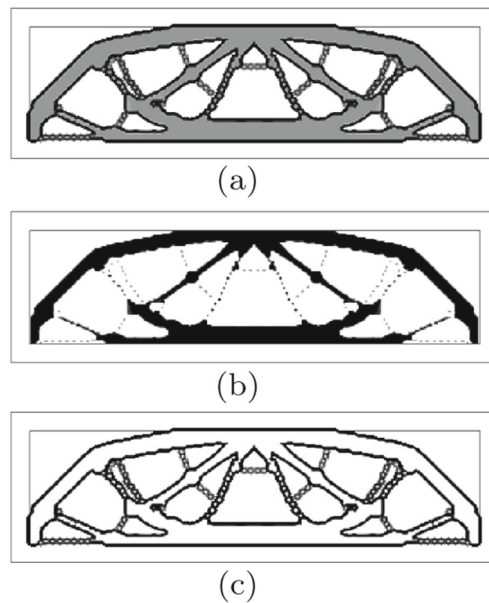


Fig. 17 Optimization result with 3-pixel coating and $E_{coating} = 2 \text{ N/m}^2$. **a** The optimized design (compliance= 50.1400 J (24.0620 J from the substrate, 26.0780 from the coating), $E_{substrate}= 1 \text{ N/m}^2$, $E_{coating}= 2 \text{ N/m}^2$, $p= 6$, $a= -30$, $b= 0.5$, $V^0= 30\%$), **b** the substrate structure, and **c** the coating structure (coating thickness=0.0333 m or 3 pixels)

In the above problems, Young's modulus of the coating structure is set to 0.1 N/m^2 with different coating thickness values; the contribution of the coating layers is less than 14%. These results show that the present coating filtering is effective for designing the coating structure in topology optimization. To test the effect of the stiffness of the coating layer, Fig. 17 shows the optimal layout for the beam problem with uniform thickness coating with $E_{coating}= 2 \text{ N/m}^2$. The overall layout is similar to the design with $E_{coating}= 0.1 \text{ N/m}^2$ but with some detail differences. In Fig. 17b and c, some interesting geometric features (named as the cheetah pattern here) with small dots representing the substrate structure and the surrounding coating structures can be observed. The dotted structure in the substrate

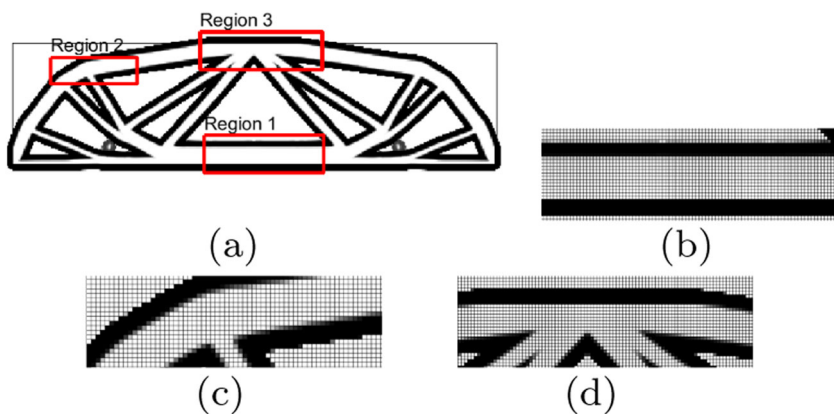
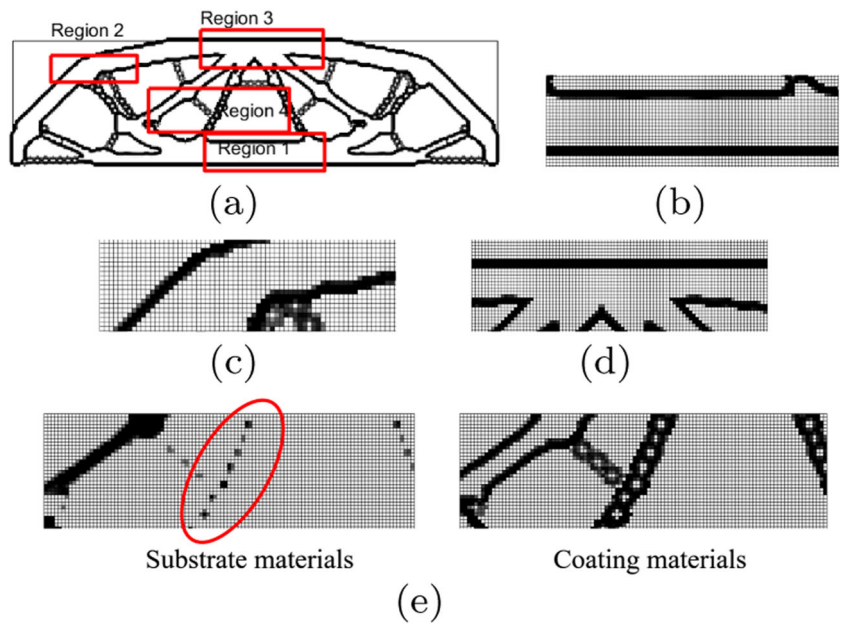


Fig. 18 Details of Fig. 17 with the coating with 3 pixels: **a** regions of interest, **b** detail of region 1, **c** the detail of region 2, **d** detail of region 3, and **e** detail of region 4



material appears and the associated coating structure emerges alongside the substrate material in Fig. 18e as the local stiffness value of the composite structure (substrate structure and coating structure) and its contribution to the global compliance becomes significant. Although these patterns appear to be another type of the checkerboard pattern caused by the finite element analysis error, they appear due to the benefit in terms of the stiffness. This phenomenon becomes significant for the truss members whose stiffness for the compression or tension force is important, as shown in Fig. 19. Indeed, the optimizer distributes the small dots to develop a repeated substrate structure and the coating structure, as shown in region 4 of Fig. 18. This result shows that the presented optimization algorithm can reflect the physical phenomenon in consideration of the stiffness of the outer structure (coating structure). These cheetah patterns become dominant with a thicker coating structure as illustrated in Fig. 20 and Fig. 21.

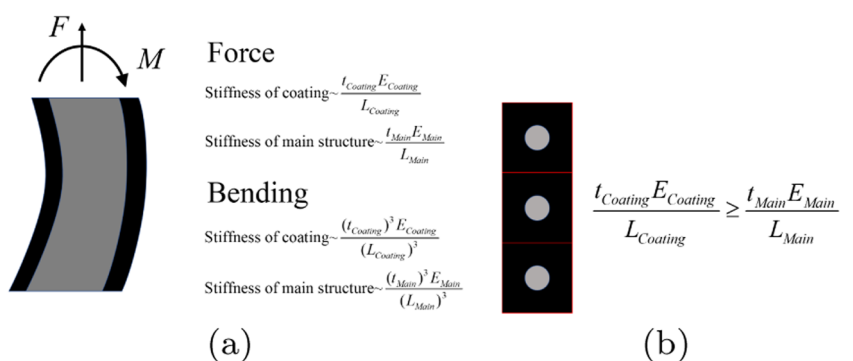
Figures 22 and 23 show the optimal layouts with $E_{coating} = 100 \text{ N/m}^2$ and $E_{coating} = 1000 \text{ N/m}^2$, respectively. Because the stiffness of the coating layer increases, the

cheetah pattern appears more clearly. To the best of our knowledge, the cheetah pattern is not related to the accuracy of the finite element method such as the checkerboard pattern or the hinge pattern. From the manufacturing viewpoint, this pattern can be cumbersome. To resolve this issue, the penalization of the cheetah pattern is required. In the present study, we tested the following optimization formulation with the perimeter of the substrate, i.e., $\|\nabla\gamma\|$ (Wang and Kang 2018). With this formulation, it is possible to find out one of the Pareto optima suppressing the appearance of the cheetah pattern.

$$\begin{aligned} \text{Min}_{\gamma} &= \mathbf{F}^T \mathbf{U} + \alpha \|\nabla\gamma\| \\ \text{Subject to } V &\leq V^0 \end{aligned} \quad (17)$$

where the weighting factor is denoted by α . By solving the above optimization formulation, the complex boundary of the substrate or the perimeter can be penalized and it is possible to obtain an optimal design with a less complex pattern. To test this formulation, the example in Fig. 23 is solved with a value of 0.2 for α . With the inclusion of this

Fig. 19 Appearance of the cheetah pattern (the dotted structure and the surrounding structure)



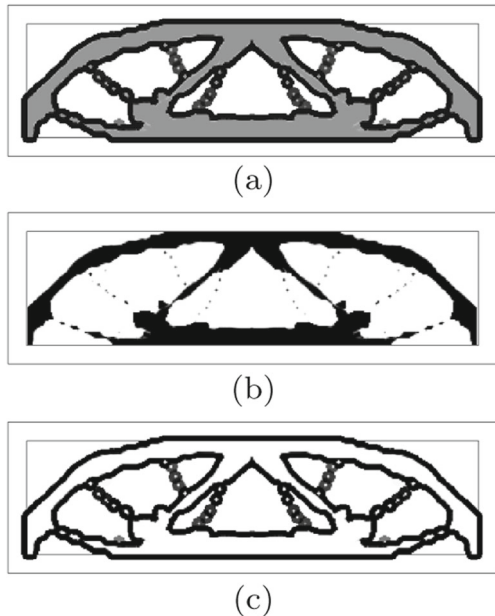


Fig. 20 Optimization result with 5-pixel coating and $E_{coating} = 2 \text{ N/m}^2$. **a** The optimized design (compliance= 39.8375 J (15.5014 J from the substrate, 24.3361 J from the coating), $E_{substrate} = 1 \text{ N/m}^2$, $E_{coating} = 2 \text{ N/m}^2$, $p = 6$, $a = -30$, $b = 0.5$, $V^0 = 30\%$), **b** the substrate structure, and **c** the coating structure (coating thickness= 0.0556 m or 5 pixels)

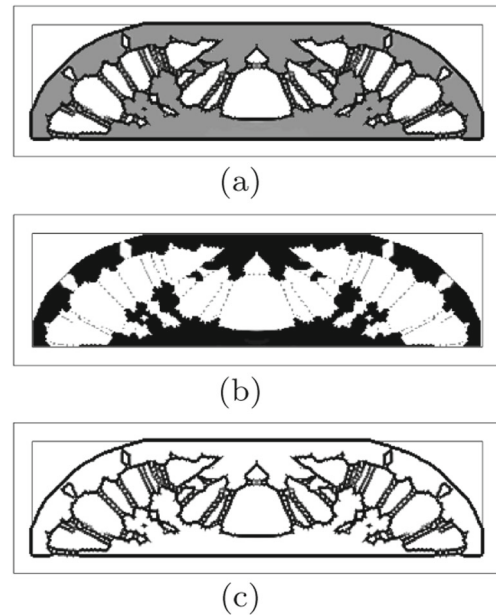


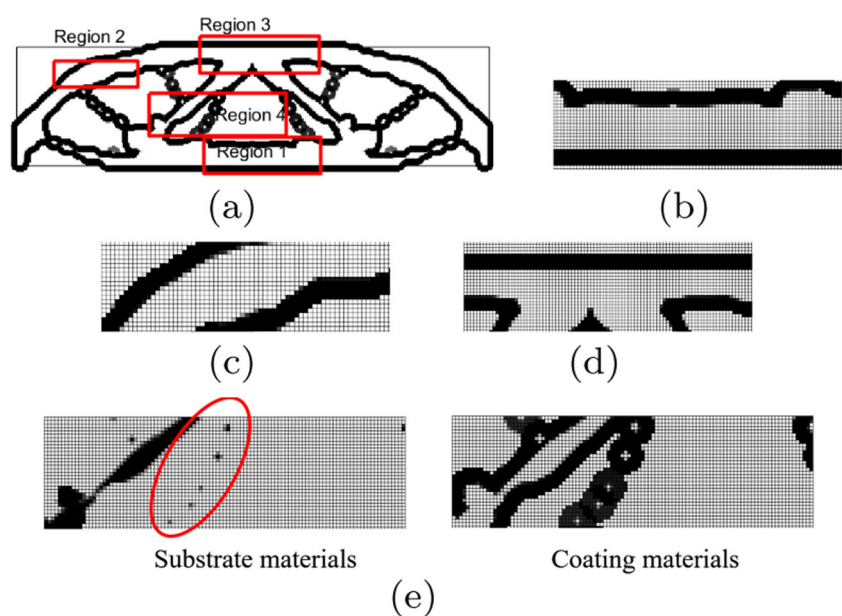
Fig. 22 Optimization result with 3-pixel coating and $E_{coating} = 100 \text{ N/m}^2$. **a** The optimized design (compliance= 4.6531 J (2.1796 J from the substrate and 2.4735 J from the coating), $E_{substrate} = 1 \text{ N/m}^2$, $E_{coating} = 100 \text{ N/m}^2$, $p = 6$, $a = -30$, $b = 0.5$, $V^0 = 30\%$, the mass of the coating= 28.0031 %), **b** the substrate structure, and **c** the coating structure (coating thickness= 0.0333 m or 3 pixels)

perimeter in the objective function, the solution in Fig. 24 without the cheetah pattern can be obtained but with 2.3969 J for the compliance higher than the original compliance, 1.3790 J.

As discussed in the previous section, the inner coating scheme can also be applied using the present filtering

scheme in Fig. 2. Figures 25 and 26 show the optimized designs with the inner coating filter. The optimizer designs the sparse truss-like structures and the inner coating structures to minimize the objective function. Unlike the outer coating scheme, the mass constraint enforces the total mass of the substrate and the coating structures.

Fig. 21 Some details of Fig. 17 with the coating with 5 pixels: **a** regions of interest, **b** detail of region 1, **c** detail of region 2, **d** detail of region 3, and **e** detail of region 4



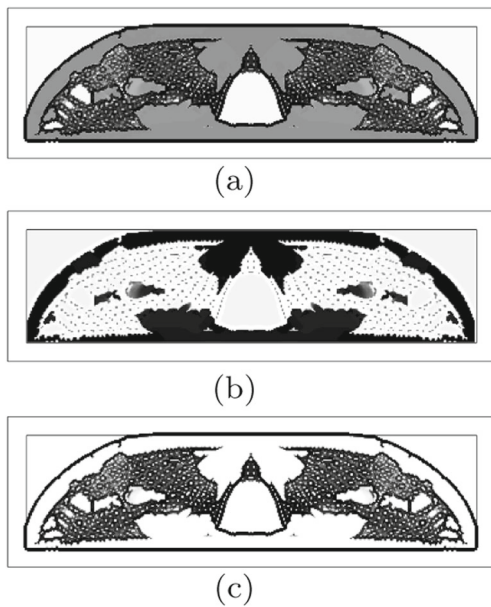


Fig. 23 Optimization result with 3 pixel and $E_{coating} = 1000 \text{ N/m}^2$. **a** The optimized design (Compliance= 1.3790 J (0.8816 J from the substrate and 0.4974 J from the coating), $E_{substrate} = 1 \text{ N/m}^2$, $E_{coating} = 1000 \text{ N/m}^2$, $p=6$, $a=-30$, $b=0.5$, $V^0 = 30\%$ the mass of the coating= 41.2623%), **b** the substrate structure, and **c** the coating structure (coating thickness= 0.0333 m or 3 pixels)

3.2 Example 2: cantilever beam problem

For the second example, the cantilever beam problem in Fig. 27 is solved with the present coating filtering scheme.

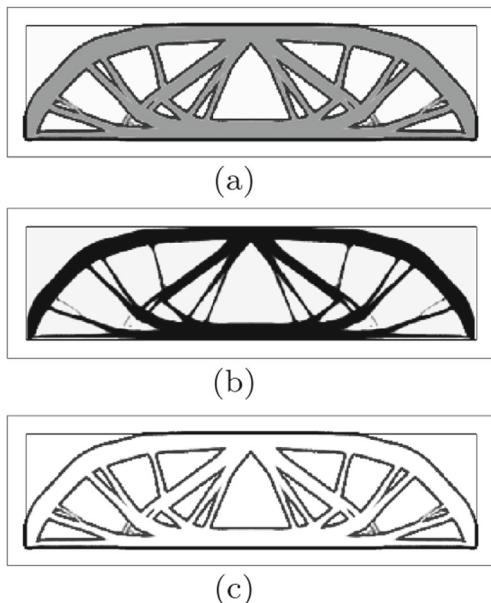


Fig. 24 The box example of Fig. 23 with the perimeter of the optimization formulation in (17). **a** The optimized design (compliance= 2.3969 J (1.6805 J from the substrate and 0.7163 J from the coating)), **b** the substrate structure, and **c** the coating structure (coating thickness= 0.0333 m or 3 pixels)

The optimization processes are carried out with different Young's moduli and a 3-pixel coating layer, as shown in Fig. 28. As observed in the first example, the present coating filter scheme successfully finds out the coating structure, as well as the inner substrate structure, by minimizing the compliance. With a higher stiffness value for the coating layer, the repeated cheetah patterns can also be found in the designs (Fig. 28b and c). Depending on the values of the stiffness of the coating layers, the compliances are changed dramatically. Note that the compliance minimization problem with coating has several local optima and the material distributions at the first optimization iterations are important in terms of the optimized layout with the coating structure.

3.3 Example 3: a rectangular domain with pressure load

For the last example, the rectangular domain ($1 \text{ m} \times 1 \text{ m}$ and the outer domain for the coating layer) with the uniform pressure load at the top surface of the domain in Fig. 29 is solved. The thickness of the outer domain of the design domain is set to 5 pixels or 0.0168 m. The optimization results with 3-pixel and 5-pixel coating layers are presented in Figs. 30 and 31, respectively. The optimization formulation is also minimizing the compliance subject to the mass constraint of the substrate structure. All examples show that the substrate structures are coated with the prescribed thickness coating layers. When the stiffness of the coating structure with a lower Young modulus is comparably low, the optimal layouts without the cheetah pattern can be obtained. By increasing the stiffness value of the coating layer or Young's modulus, the cheetah patterns appear again. With an extreme case with 1000 N/m^2 , the entire domain is filled with the cheetah patterns (Fig. 31c). We observe that the “coating” or the related structure or technique in the industry does not consider the stiffness of the coating layer and it is common to design without considering the stiffness contribution of the coating layer to the substrate structure. After finishing the detailed design for the substrate structure, a very thin coating layer, with negligible stiffness, is added to protect the corrosion and the erosion. When the stiffness contribution of the coating layer cannot be negligible, we should consider the stiffness effect of the coating layer. The current optimization scheme can then be used to design an optimal layout considering the coating layer stiffness.

4 Conclusions

The present study develops a new density filter for the coating and presents its usage for structural topology

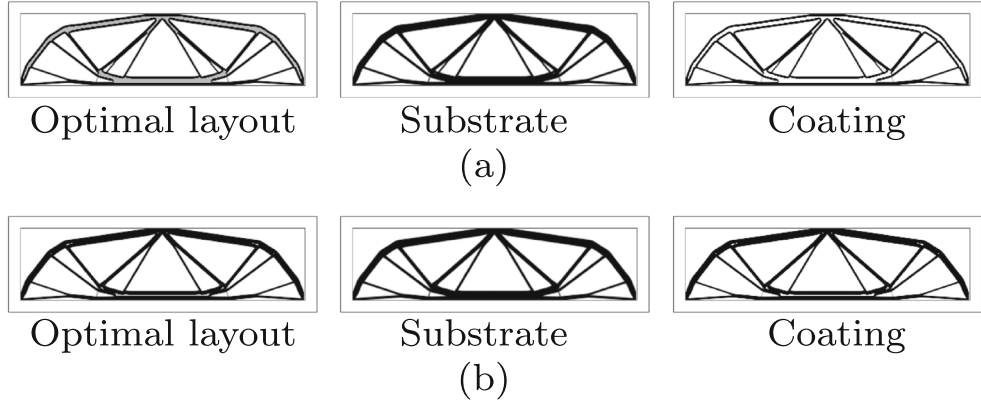


Fig. 25 The box example with the inner coating filter ($E_{substrate} = 1 \text{ N/m}^2$, $E_{coating} = 0.1 \text{ N/m}^2$, $p = 6$, $a = -30$, $b = 0.5$, $V^0 = 30\%$). **a** An optimal design with coating thickness= 0.0333 m or 3 pixels (compliance= 119.0542 J, the mass of the substrate= 10.6133 %, the mass of

the coating= 19.3867%) and **b** an optimal design with coating thickness= 0.0556 m or 5 pixels (compliance= 116.1250 J, the mass of the substrate= 3.7887 %, the mass of the coating= 26.2113%)

optimization minimizing the compliance subject to the mass constraint. The consideration of the manufacturing constraint becomes important in topology optimization research and we regard the topology optimization with the coating as an optimization with a special manufacturing constraint (an optimization considering the stiffness effect of the coating layer). The coating structure does not mean that the uniform thickness is simply added on the surface of the substrate structure. Rather, the stiffness effect of the coating layer should be considered during the optimization. However, its realization in topology optimization is a difficult job. This study develops a new density coating filter approach to consider the coating structure. Compared to the other approaches, this density coating filter uses a simple averaging or the p -norm of the neighborhood densities for the envelope with a constant thickness and we propose to multiply the modified density and the inverted density, i.e.,

$1 - \gamma$, to define the coating layer. By changing the design variable to the inverted design variable, the inner coating scheme is also developed. Three compliance minimization problems are solved to demonstrate the validity and effectiveness of the present coating filter. The designs obtained with the coating filter suggest that the present approach enables us to efficiently obtain optimal layouts with the coating structure. Depending on the magnitude of Young's modulus of the coating structure and the prescribed thickness, the ratio of the strain energies of the substrate and the coating varies dramatically; in some conventional coating applications to hazard environment, the stiffness contribution of the coating layer is negligible. As the present coating filter is based on the size of the finite element mesh, the optimized layouts are dependent on the mesh. In the future, the extension of the coating scheme for irregular meshes or shell elements can be conducted.

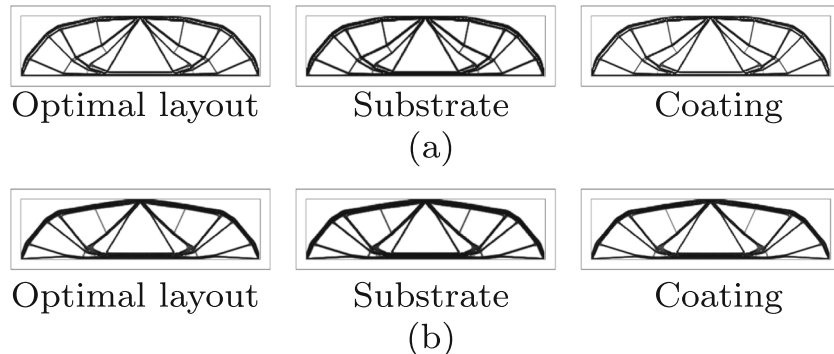


Fig. 26 The box example with the inner coating filter ($E_{substrate} = 1 \text{ N/m}^2$, $E_{coating} = 1000 \text{ N/m}^2$, $p = 6$, $a = -30$, $b = 0.5$, $V^0 = 30\%$). **a** An optimal design with coating thickness= 0.0333 m or 3 pixels (compliance= 0.1724 J, the mass of the substrate= 6.2681 %, the mass of the

coating= 23.7319%) and **b** an optimal design with coating thickness= 0.0556 m or 5 pixels (compliance= 0.1520 J, the mass of the substrate= 4.8821 %, the mass of the coating= 25.1179 %)

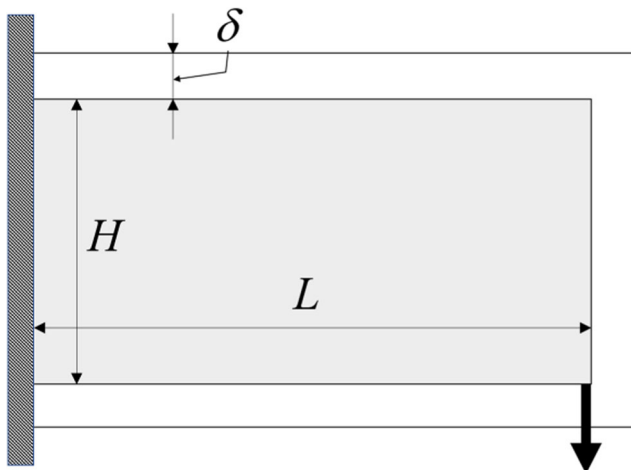


Fig. 27 The cantilever problem definition ($L = 2$ m, $H = 1$ m, thickness = 1 m, $\delta = 0.3330$ m, $F = 1$ N, 180×90 discretization, densities of the substrate and the coating = 1 kg/m^3)

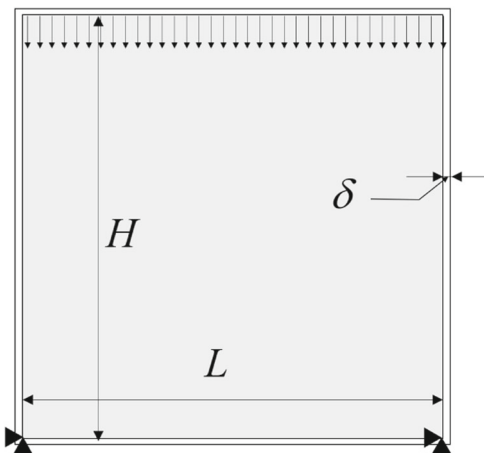


Fig. 29 Pressure example with the coating filter (a problem definition $L = 1$ m, $H = 1$ m, thickness = 1 m, $\delta = 0.0333$ m, pressure = 300 N/m^2 , 300×300 discretization, densities of the substrate and the coating = 1 kg/m^3)

5 Replication of results

In order to help understand the content and replicate the results, a code (coating.m) and an example file are available

as supplementary material for the filtering in Fig. 5. After the understanding the coating approach, the finite element analysis, the sensitivity analysis, and the optimization process can be implemented.

Fig. 28 Cantilever example with the coating filter ($E_{\text{substrate}} = 1 \text{ N/m}^2$, $p = 6$, $a = -30$, $b = 0.5$, $V^0 = 30\%$, coating thickness = 0.0333 m or 3 pixels). **a** An optimal design ($E_{\text{coating}} = 0.1 \text{ N/m}^2$, compliance = 104.6716 J, the mass of the coating = 19.6050 %), **b** an optimal design ($E_{\text{coating}} = 100 \text{ N/m}^2$, compliance = 3.2124 J, the mass of the coating = 24.3407 %), and **c** an optimal design ($E_{\text{coating}} = 1000 \text{ N/m}^2$, compliance = 0.7223 J, the mass of the coating = 23.7314 %)

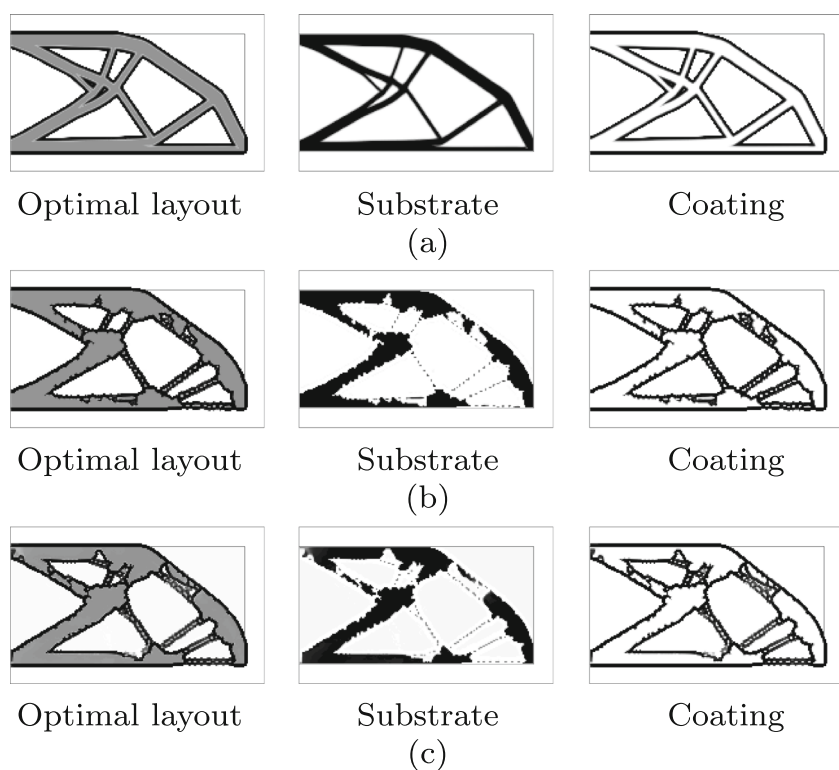


Fig. 30 Optimization results with 3-pixel coating layer ($E_{substrate} = 1 \text{ N/m}^2$, $p = 6$, $a = -30$, $b = 0.5$, $V^0 = 30\%$). **a** An optimal design ($E_{coating} = 0.1 \text{ N/m}^2$, compliance = $3.8619 \times 10^5 \text{ J}$, the mass of the coating = 11.5626%), **b** an optimal design ($E_{coating} = 2 \text{ N/m}^2$, compliance = $1.9555 \times 10^5 \text{ J}$, the mass of the coating = 10.5507%), and **c** an optimal design ($E_{coating} = 1000 \text{ N/m}^2$, compliance = $4.3817 \times 10^3 \text{ J}$, the mass of the coating = 32.6268%)

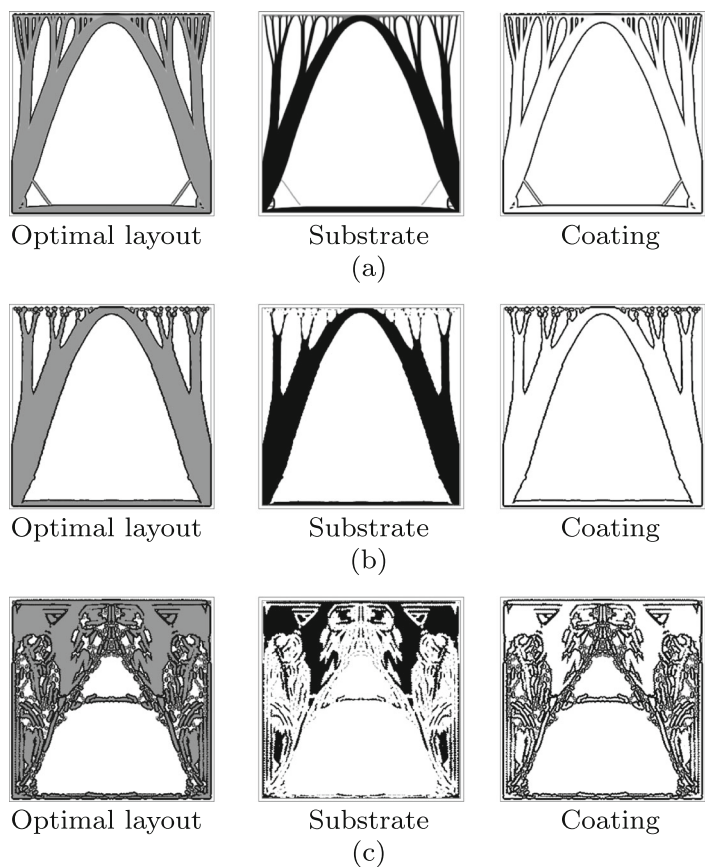
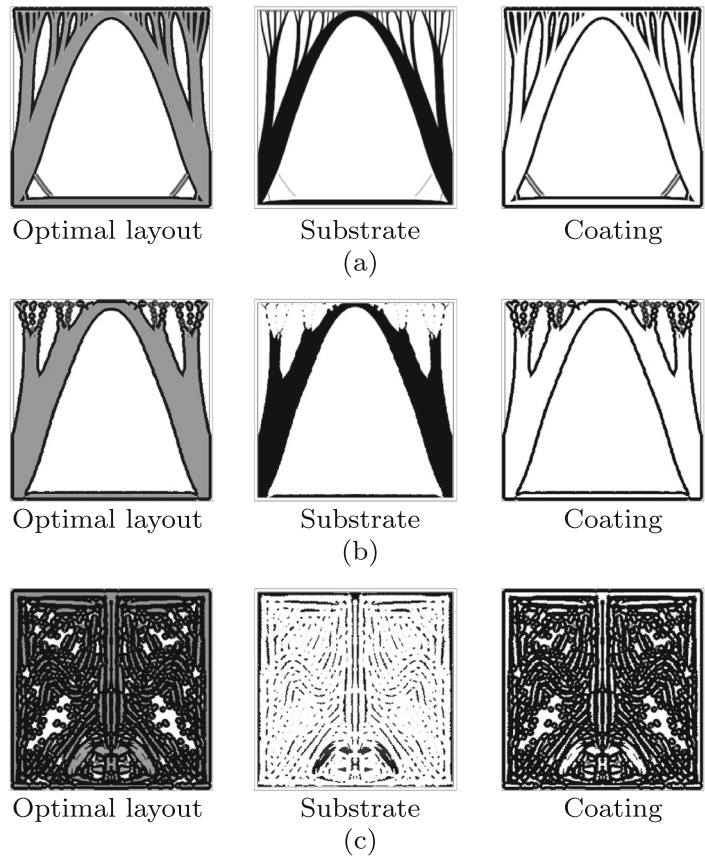


Fig. 31 The optimization results with 5-pixel coating layer ($E_{substrate} = 1 \text{ N/m}^2$, $p = 6$, $a = -30$, $b = 0.5$, $V^0 = 30\%$, coating thickness=0.0556 m or 5 pixels, densities of the substrate and the coating = 1 kg/m^3). **a** An optimal design ($E_{coating} = 0.1 \text{ N/m}^2$, compliance = $3.6913 \times 10^5 \text{ J}$, the mass of the coating = 19.6050%), **b** an optimal design ($E_{coating} = 2 \text{ N/m}^2$, compliance = $1.5590 \times 10^5 \text{ J}$, the mass of the coating = 24.3407%), and **c** an optimal design ($E_{coating} = 1000 \text{ N/m}^2$, compliance = $1.0266 \times 10^3 \text{ J}$, the mass of the coating = 23.7314%)



Acknowledgments This work was supported by the National Research Foundation of Korea (NRF) grant funded by the Korea government (MSIT)(No.2018R1A5A7025522).

Compliance with ethical standards

Conflict of interests The authors declare that they have no conflict of interest.

References

- Alexandersen J, Aage N, Andreasen CS, Sigmund O (2012) Topology optimisation for natural convection problems. *Int J Numer Methods Fluids* 76(10):699–721
- Bendsøe M, Kikuchi N (1988) Generating optimal topologies in structural design using a homogenization method. *Comput. Methods Appl Mech Eng* 71(2):197–224
- Clausen A, Aage N, Sigmund O (2015) Topology optimization of coated structures and material interface problems. *Comput. Methods Appl Mech Eng* 290:524–541
- Deaton JD, Grandhi RV (2014) A survey of structural and multidisciplinary continuum topology optimization: post 2000. *Struct Multidiscip Optim* 49(1):1–38
- Dede EM, Lee J, Nomura T (2014) Multiphysics simulation: electromechanical system applications and optimization. Springer, London
- Evgrafov A, Pingen G, Maute K (2008) Topology optimization of fluid domains: kinetic theory approach. *ZAMM - J Appl Math Mech / Zeitschrift für Angewandte Mathematik und Mechanik* 88:129–141
- Fu J, Li H, Xiao M, Gao L, Chu S (2019) Topology optimization of shell-infill structures using a distance regularized parametric level-set method. *Struct Multidiscip Optim* 59(1):249–262. <https://doi.org/10.1007/s00158-018-2064-6>
- Fu J, Li H, Gao L, Xiao M (2019) Design of shell-infill structures by a multiscale level set topology optimization method. *Comput Struct* 212:162–172
- Ha SH, Cho S (2005) Topological shape optimization of heat conduction problems using level set approach. *Numerical Heat Transfer, Part B: Fundamentals* 48(1):67–88
- Jensen J, Sigmund O (2011) Topology optimization for nanophotonics. *Laser Photonics Rev* 5(2):308–321
- Langelaar M (2016) Topology optimization of 3d self-supporting structures for additive manufacturing. *Addit Manuf* 12:60–70
- Langelaar M (2018) Combined optimization of part topology, support structure layout and build orientation for additive manufacturing. *Struct Multidiscip Optim* 57(5):1985–2004. <https://doi.org/10.1007/s00158-017-1877-z>
- Li Q, Chen W, Liu S, Tong L (2016) Structural topology optimization considering connectivity constraint. *Struct Multidiscip Optim* 54(4):971–984
- Lu L, Sharf A, Zhao H, Wei Y, Fan Q, Chen X, Savoye Y, Tu C, Cohen-Or D, Chen B (2014) Build-to-last: strength to weight 3d printed objects. *ACM Trans Graph (Proc SIGGRAPH)* 33(4):97:1–97:10
- Møller P, Nielsen L (2013) Advanced Surface Technology, vol 1–2. Møller & Nielsen
- Moon SJ, Yoon GH (2013) A newly developed qp-relaxation method for element connectivity parameterization to achieve stress-based topology optimization for geometrically nonlinear structures. *Comput Methods Appl Mech Eng* 265:226–241. <https://doi.org/10.1016/j.cma.2013.07.001>, <http://www.sciencedirect.com/science/article/pii/S004578251300162X>
- Papoutsis-Kiachagias EM, Giannakoglou KC (2016) Continuous adjoint methods for turbulent flows, applied to shape and topology optimization: industrial applications. *Arch Comput Meth Eng* 23(2):255–299
- Sato Y, Yamada T, Izui K, Nishiwaki S (2017) Manufacturability evaluation for molded parts using fictitious physical models, and its application in topology optimization. *Int J Adv Manuf Technol* 92(1):1391–1409
- Schaedler TA, Jacobsen AJ, Torrents A, Sorensen AE, Lian J, Greer JR, Valdevit L, Carter WB (2011) Ultralight metallic microlattices. *Science* 334(6058):962–965
- Shchukin D, Möhwald H (2013) A coat of many functions. *Science* 341(6153):1458–1459
- Svanberg K (1987) The method of moving asymptotes – a new method for structural optimization. *Int J Numer Methods Eng* 24(2):359–373
- Tofail SAM, Koumoulos EP, Bandyopadhyay A, Bose S, O'Donoghue L, Charitidis C (2018) Additive manufacturing: scientific and technological challenges, market uptake and opportunities. *Mater Today* 21(1):22–37
- Tsuji Y, Hirayama K, Nomura T, Sato K, Nishiwaki S (2006) Design of optical circuit devices based on topology optimization. *IEEE Photon Technol Lett* 18(7):850–852
- Wang MY, Wang X, Guo D (2003) A level set method for structural topology optimization. *Comput Methods Appl Mech Eng* 192(1):227–246
- Wang W, Wang TY, Yang Z, Liu L, Tong X, Tong W, Deng J, Chen F, Liu X (2013) Cost-effective printing of 3d objects with skin-frame structures. *ACM Trans Graph* 32(6):177:1–177:10
- Wang Y, Kang Z (2018) A level set method for shape and topology optimization of coated structures. *Comput. Methods Appl Mech Eng* 329:553–574
- Wang H, Chen Y, Rosen DW (2005) A hybrid geometric modeling method for large scale conformal cellular structures. In: ASME. International design engineering technical conferences and computers and information in engineering conference, vol 3: 25th computers and information in engineering conference, parts A and B, pp 421–427. <https://doi.org/10.1115/DETC2005-85366>
- Wu J, Clausen A, Sigmund O (2017) Minimum compliance topology optimization of shell-nfill composites for additive manufacturing. *Comput Methods Appl Mech Eng* 326:358–375
- Wu J, Aage N, Westermann R, Sigmund O (2018) Infill optimization for additive manufacturing—approaching bone-like porous structures. *IEEE Trans Vis Comput Graph* 24(2):1127–1140
- Xia Q, Shi T, Liu S, Wang MY (2012) A level set solution to the stress-based structural shape and topology optimization. *Comput Struct* 90–91:55–64. <https://doi.org/10.1016/j.compstruc.2011.10.009>, <http://www.sciencedirect.com/science/article/pii/S0045794911002562>
- Xie Y, Steven G (1993) A simple evolutionary procedure for structural optimization. *Comput Struct* 49(5):885–896
- Yoon GH (2010) Topological design of heat dissipating structure with forced convective heat transfer. *J Mech Sci Technol* 24(6):1225–1233
- Yoon GH (2012) Topological layout design of electro-fluid-thermal-compliant actuator. *Comput. Methods Appl Mech Eng* 209–212:28–44
- Yoon GH (2013) Acoustic topology optimization of fibrous material with delany–bazley empirical material formulation. *J Sound Vib* 332(5):1172–1187
- Yoon GH (2014) Stress-based topology optimization method for steady-state fluid–structure interaction problems. *Comput Methods Appl Mech Eng* 278:499–523. <https://doi.org/10.1016/j.cma.2014.05.021>, <http://www.sciencedirect.com/science/article/pii/S0045782514001820>

- Yoon GH (2016) Topology optimization for turbulent flow with spalart–allmaras model. *Comput Methods Appl Mech Eng* 303:288–311
- Yoon GH, Kim YY (2003) The role of s-shape mapping functions in the simp approach for topology optimization. *KSME Int J* 17(10):1496–1506
- Yu Y, Hur T, Jung J, Jang IG (2019) Deep learning for determining a near-optimal topological design without any iteration. *Struct Multidiscip Optim* 59(3):787–799. <https://doi.org/10.1007/s00158-018-2101-5>
- Zhang W, Li D, Zhou J, Du Z, Li B, Guo X (2018) A moving morphable void (mmv)-based explicit approach for topology optimization considering stress constraints. *Comput. Methods Appl Mech Eng* 334:381–413. <https://doi.org/10.1016/j.cma.2018.01.050>, <http://www.sciencedirect.com/science/article/pii/S0045782518300574>

Publisher's note Springer Nature remains neutral with regard to jurisdictional claims in published maps and institutional affiliations.